Synchronization of indirect and direct three coupled lasers in a ring

M S Mahmoud, M Medhat, and Hassan F El-Nashar*

Physics Department, Faculty of Science, Ain Shams University, Cairo 11566, Egypt.

We investigated systems of three non-identical lasers coupled to each other in a ring topology. We introduced the coupling mechanism between the two lasers by direct and indirect coupling methods. In the weak coupling limit, a stable phase lock between lasers occurred at a critical coupling value. The analytic method revealed that the coupled lasers are described by a model which showed an amplitude and a phase dependence, for the first method of coupling. Also, the methodical investigations indicated that the coupled lasers in the second method of coupling are depicted by a coupled phase model only. Synchronization appeared in both methods at critical coupling constants. However, the synchronization mechanisms in the direct and indirect coupled lasers are interpreted in different ways. The unison behavior appeared at a small coupling constant for the indirect coupling technique in comparison to the case having the same conditions of the direct coupling technique.

Keywords

1. Introduction

Fathoming the synchronization phenomenon in many systems in nature is a challenging problem. It plays a crucial role in physics, chemistry, engineering, biology and social sciences [1-9]. Specifically, in physics of optical systems, coherent beam combining of several non-identical lasers can result in high power levels and better beam quality [6]. This process can be obtained by introducing a suitable coupling between the small-detuned lasers to synchronize their frequencies to a common value. A phase lock between two lasers of dissimilar frequencies exists by coupling them through a partially transmitting window, at a critical coupling [10]. By increasing the number of coupled lasers, synchronization of an array of class B lasers coupled by a local method in a ring and in a global coupled technique, are described by a local and global Kuramoto model [11], respectively. Recently, The Kuramoto model provides a successful explanation of coupled lasers [11-14].

A quantitative analysis of reaching the common frequency value requires starting from three lasers because this configuration is a borderline between the local and global coupled lasers [17, 18]. Upon understanding the synchronization of three coupled lasers, we can extend the method later to a larger number of lasers than three. Thus, we shall demonstrate the mechanisms of synchronization in both connectivity methods. Direct coupling between two lasers is achieved by placing the resonators in proximity to each other in a ring topology [14]. On the other hand, the indirect coupling is attained by inserting a passive cavity between two lasers to make them coupled in a ring [13, 14]. The two methods show different dynamical features to observe the frequency synchronization at a critical coupling.

In the current work, we introduce the problem of coupled three laser resonators in a ring topology by two methods: Direct and indirect couplings. We study these systems analytically and we show that in the case of the direct coupling, the three lasers are represented by a model (phase and amplitude dependence) where synchronization appears as frequencies dependence without any general phase lock solution. Also, the common frequency is not given by a unique expression. In the indirect coupling case, we find the connected lasers are expressed by a phase model only. It is possible to find analytic expressions for the critical coupling constant (at a phase lock). Furthermore, analytic relations are found for the phase differences between each two lasers.

This work is organized as follows: in section. 2, we investigate the system of three directly coupled lasers in a ring. In section. 3, we investigate the system of three lasers coupled to each other in a ring by an indirect interaction. A conclusion is given in sections. 4 and 5.

2. Three directly coupled lasers in a ring.

The laser (classes A and B) is a nonlinear dynamical system that can be described as a limit cycle oscillator [11-14]. The laser has three degrees of freedom, the electric field amplitude, the atomic inversion density, and atomic polarization. For class B lasers, the polarization degree of freedom relaxes faster than the other two degrees of freedom. In addition, the dynamics of the atomic inversion density becomes constant depending on the threshold [14-16]. In class A lasers, the atomic inversion density as well as the atomic polarization relax faster than the electric field [11-16]. Therefore, for both classes (A and B), the time evolution of polarization and the time evolution of the atomic inversion density are eliminated. Henceforward, for classes A and B, the dynamics of the electric field is described by a Stuart-Landau oscillator [13, 19]. Consequently, the field amplitude dynamics of the laser is written as [13, 19]:

$$\frac{d\alpha}{dt} = -i\omega\alpha + \frac{\kappa}{2}(\epsilon - 1)\alpha - \frac{\kappa}{2}\beta\,|\alpha|^2\alpha. \qquad (1)$$

In equation (1), α is the electric field amplitude, the laser field has frequency ω and a photon decay rate κ. The spontaneous emission rate is β. The pump power is P and the threshold pump value is $P_{th}= \kappa/\beta$. The parameter ϵ is the pump parameter with $\epsilon = P_{th}/P$. The. The limit cycle solution of equation (1) is $((\epsilon - 1)/\beta)^{1/2}$ [13, 19].

Figure 1.a shows the direct three coupled lasers. The coupling allows photons to be exchanged between adjacent oscillators bidirectionally. For the three coupled lasers in a ring, as shown in figure 1.a, each laser amplitude is α_j with a decay rate κ and pump parameter ϵ. The three lasers L_1, L_2 and L_3 are identical except for their frequencies.
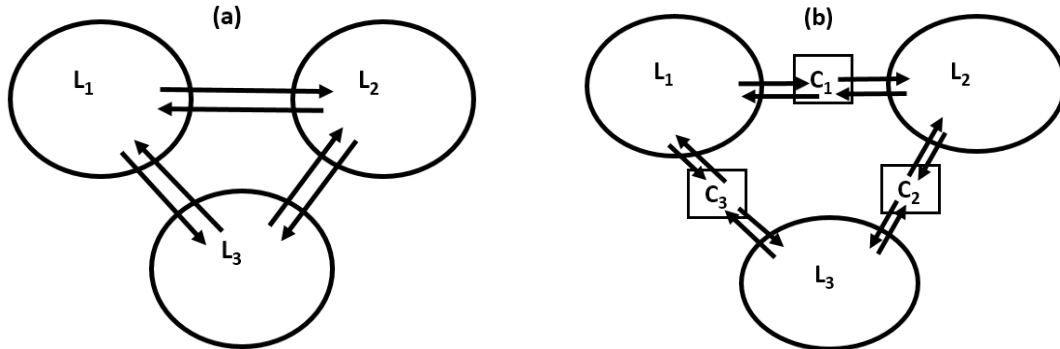

Figure 1. Schematic diagram of three coupled lasers in a ring topology. The arrows indicate directions of exchanging photons. (a) The lasers L_1, L_2 and L_3 are coupled by placing the three cavities in proximity. (b) The indirect coupling is established by placing three cold cavities C_1, C_2 and C_3 between each two adjacent lasers.

The governing dynamics can be written as [13, 19]:

$$\dot{\alpha}_j = -i\omega_j\alpha_j + \frac{\kappa}{2}(\epsilon - 1)\alpha_j - \frac{\kappa}{2}\beta|\alpha_j|^2\alpha_j - \frac{i\sigma}{3}(\alpha_{j+1} + \alpha_{j-1}), \qquad (2)$$

for j =1, 2, 3. The periodic boundary conditions demand $i \pm 3 = i$. In equation (2), σ is the coupling constant. Utilize $\alpha_j = \rho_j(t)e^{-i\theta_j(t)}$, we write the amplitude and phase evolution according to system (2), for j =1, 2, 3, as:

$$\dot{\rho}_j = \left(\frac{\kappa}{2}(\epsilon - 1) - \frac{\kappa}{2}\beta\rho_j{}^2\right)\rho_j - \frac{\sigma}{3}\left(\rho_{j+1}\sin(\theta_j - \theta_{j+1}) + \rho_{j-1}\sin(\theta_j - \theta_{j-1})\right), \quad (3.a)$$

$$\dot{\theta}_j = \omega_j + \frac{\sigma}{3}\left(\frac{\rho_{j+1}}{\rho_j}\cos(\theta_j - \theta_{j+1}) + \frac{\rho_{j-1}}{\rho_j}\cos(\theta_j - \theta_{j-1})\right). \quad (3.b)$$

where ρ_j and θ_j are a real amplitude and a phase of each laser, for j =1, 2, 3. The coupling constant between two nearest neighbor lasers is σ. Thus, the direct coupling indicates dependence of the time evolution of amplitudes and phases on both phases and amplitudes ρ_j and θ_j. Relations (3) indicate that upon increasing the value of σ, the lasers can synchronize and have a common frequency at a critical coupling σ_c. Numerical studies of equations (2.a and 3.b) reveal this fact and the results are shown in both diagrams of figure 2. We integrate (2.a and 3.b) using a time step $\Delta\tau = 0.001$. In figure 2.a we plot, at σ_c, the amplitudes and the time evolution of the amplitude versus time, where τ represents the sum of time steps $\Delta\tau$ and the time is τ rescaled by a decay rate κ of lasers. In figure 2.b we show the synchronization of the detuned lasers to a common value ω when we plot the time average of the time evolution of phases versus the coupling constant. Figure 2.a confirms that the time evolution of the amplitudes and the amplitudes become time-independent at σ_c. Besides, at σ_c, it is not possible for the amplitudes to have the same value. Therefore, for the direct coupling method, it is not

possible to express the system by the phase model only although at σ_c the phases are time independent. Thus, the phases' time evolution in (3.b) shows that the lasers can synchronize to a common frequency $\omega \neq \omega_o$, where $\omega_o = (\omega_{max} + \omega_m + \omega_{min})/3$, and the phases are locked at a critical coupling value σ_c see figure 2.b. This can be verified by adding the three phase equations in a relation (3.b), the cosinusoidal coupling functions (even functions) cannot cancel each other, which lead to

$$\omega = \omega_o + \frac{\sigma_c\left(\left(\frac{\rho_j}{\rho_{j-1}}+\frac{\rho_{j+1}}{\rho_j}\right)\cos(\theta_j-\theta_{j-1})+\left(\frac{\rho_{j+1}}{\rho_j}+\frac{\rho_j}{\rho_{j+1}}\right)\cos(\theta_{j+1}-\theta_j)+\left(\frac{\rho_{j-1}}{\rho_{j+1}}+\frac{\rho_{j+1}}{\rho_{j-1}}\right)\cos(\theta_{j-1}-\theta_{j+1})\right)}{9},$$

where, the second term in the previous relation cannot reach zero. Thus, we call this case of a direct coupling (relations (3)) a coupled phase model as amplitude-phase model.
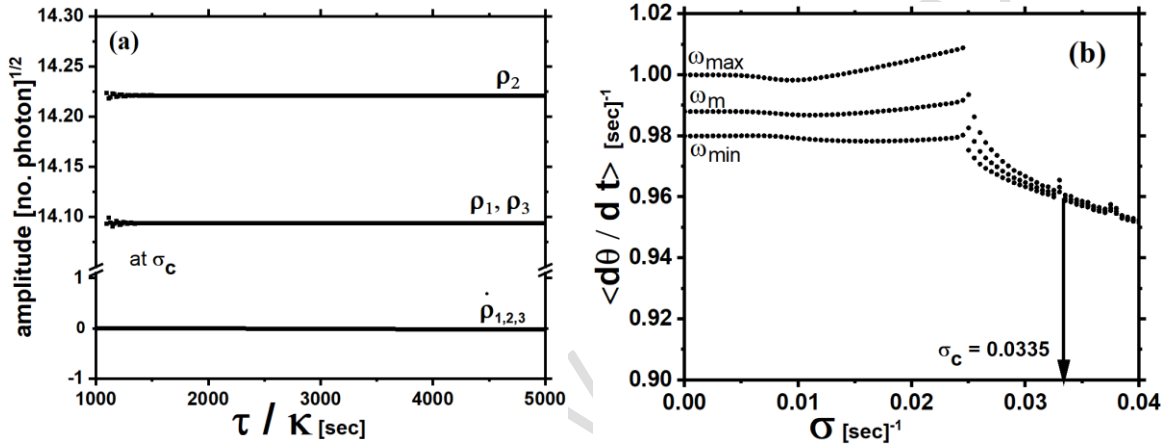

Figure 2. (a)The amplitude dissimilarity of the three directly coupled lasers at the critical coupling constant. Each amplitude becomes time independent at σ_c. (b) Bifurcation diagram for the average instantaneous phases plotted against the coupling constant σ. In this figure, we used $\omega_{max} = 1\, rad/s$, $\omega_m = 0.988\, rad/s$, and $\omega_{min} = 0.98\, rad/s$ with $\kappa = 100\ s^{-1}$, $\beta = 0.001\ s^{-1}$ and $\epsilon = 1.2$.

3. Three indirectly coupled lasers in a ring.

The indirect coupling is performed by placing three cold cavities adjacently between each two lasers, see figure 1. b. Figure 1.b shows the indirectly three coupled lasers L_1, L_2 and L_3 were each two lasers exchange photons through common cavities C_1, C_2 and C_3. The coupling allowing photons to be exchanged between adjacent oscillators bidirectional. The coupled field' amplitudes expressions for the three lasers are written as [12-14, 19]

$$\frac{d\alpha_i}{dt} = -i\omega_i\alpha_i + \frac{\kappa}{2}(\epsilon - 1)\alpha_i - \frac{\kappa}{2}\beta\, |\alpha_i|^2\alpha_i - \frac{ig}{3}(A_j + A_{j-1}), \qquad (4)$$

where $i = 1, 2, 3$, and $j = 1, 2, 3$. The periodic boundary conditions require $i \pm 3 = i$ and $j \pm 3 = j$. The constant g depends on the coupling strength between the lasers. For the jth cold cavity, the complex intracavity field amplitude is A_j. The intracavity field of the cold cavity is expressed by the equation [13,14]:

$$\frac{dA_j}{dt} = -i\omega_o A_j - \frac{\Gamma}{2} A_j - \frac{ig}{3}(\alpha_i + \alpha_{i+1}), \qquad (5)$$

where Γ is the photon decay rate in each cold cavity.

We choose each laser cavity parameters identical. The natural frequencies of the lasers are detuned by a very small mismatch. Employ $A_j = \mu_j(t)e^{-i\phi_j(t)}$, for j = 1, 2, 3, and $\alpha_j = \rho_j(t)e^{-i\theta_j(t)}$ for i =1, 2, 3, with $\psi_{j,i} = \phi_j - \theta_i$. Consequently, we write first the equation (5) in the polar forms, for the passive cavities, as:

$$\dot{\mu}_j = \frac{-\Gamma}{2}\mu_j + \frac{g}{3}\left(\rho_j\sin\psi_{j,j} + \rho_{j+1}\sin\psi_{j,j+1}\right), \qquad (6.a)$$

and

$$\dot{\phi}_j = \omega_0 + \frac{g}{3}\left(\frac{\rho_j}{\mu_j}\cos\psi_{j,j} + \frac{\rho_{j+1}}{\mu_j}\cos\psi_{j,j+1}\right). \qquad (6.b)$$

The nature of the passive cavities (do not contain amplifying media) does not allow $<\dot{\mu}_j>_t$ and $<\dot{\phi}_j>_t$ to fluctuate largely around their zero as well as $<\mu_j>_t=$ $constant$. Therefore, we expect, at a certain coupling constant (g_c^*), to find the amplitudes and phases of cold cavities are time independent. As a result, at values of $g<$ g_c^* we find $\dot{\mu}_j \cong 0$ and $\dot{\phi}_j \cong \omega_o$ and at g_c^* we have $\dot{\mu}_j = 0$ and $\dot{\phi}_j = \omega_o$. Also, we obtain expressions for the amplitudes' time evolution of the lasers and phases, for i =1, 2, 3, by relating the index i to the index j, as:

$$\dot{\rho}_i = \left(\frac{\kappa}{2}(\epsilon - 1) - \frac{\kappa}{2}\beta\rho_i^2\right)\rho_i - \frac{g}{3}\left(\mu_i\sin\psi_{i,i} + \mu_{i-1}\sin\psi_{i-1,i}\right), \qquad (7.a)$$

and

$$\dot{\theta}_i = \omega_i + \frac{g}{3}\left(\frac{\mu_i}{\rho_i}\cos\psi_{i,i} + \frac{\mu_{i-1}}{\rho_i}\cos\psi_{i-1,i}\right), \qquad (7.b)$$

where the over dot indicates the time evolution. Equations (6 and 7) show, in the case of the indirect coupling, the time evolution of amplitudes and phases depend on amplitudes and coupled phase quantities.
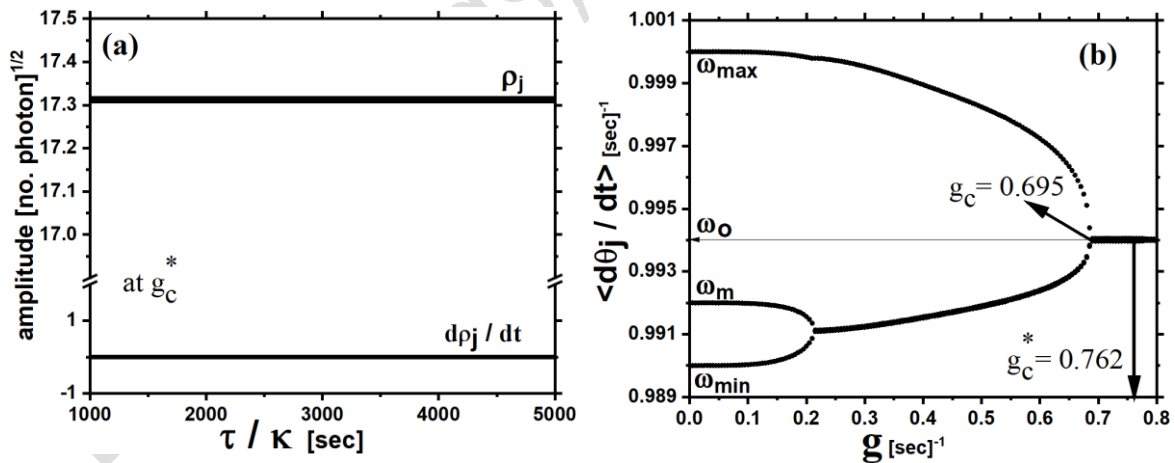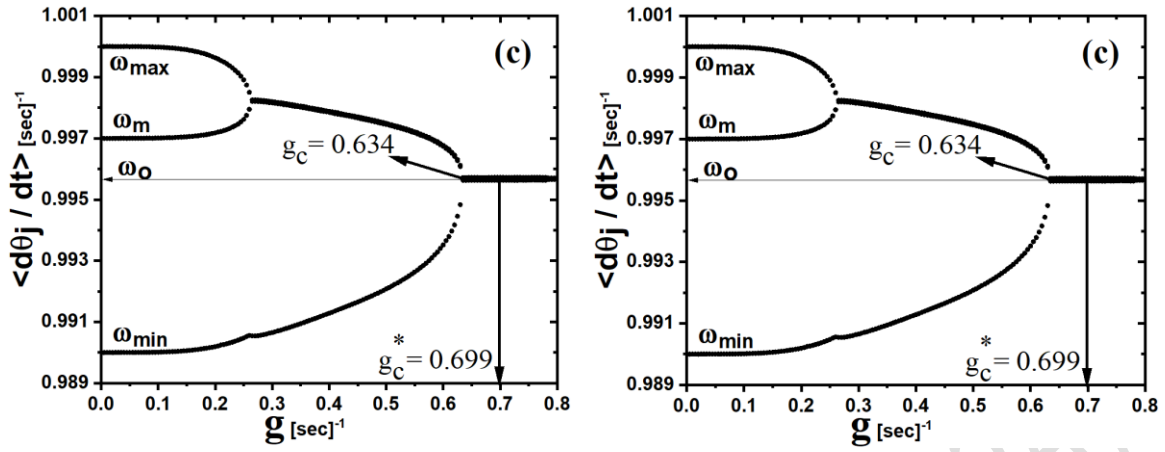
Figure 3. (a) The time independence of the three amplitudes of the lasers is shown at the critical coupling constant. The rest three plots are dedicated to the bifurcation diagrams for the lasers' instantaneous phases (averaged over time) versus the coupling constant. The data in this figure is obtained for $\kappa = 100\ s^{-1}$, $\epsilon = 1.3$, $\Gamma = 10\ s^{-1}$. (b) $\{\omega_{max}, \omega_m, \omega_{min}\} = \{1, 0.992, 0.99\}$. (c) $\{\omega_{max}, \omega_m, \omega_{min}\} = \{1, 0.997, 0.99\}$. (d) $\{\omega_{max}, \omega_m, \omega_{min}\} = \{1, 0.995, 0.99\}$. All frequencies are measured in rad/s.

Manipulate the above particulars, $\dot{\mu}_j = 0$ and $\dot{\phi}_j = \omega_o$, into equations (6.a and 6.b) we have $\mu_j = (2g/3\Gamma)(\rho_j \sin\psi_{jj} + \rho_{j+1} \sin\psi_{j,j+1})$ and $\rho_j/\rho_{j+1} = -\cos\psi_{j,j+1}/\cos\psi_{jj}$. Correspondingly, we reduce the four relations of (6 and 7) to the following expressions

$$\dot{\rho}_i = \left(\frac{\kappa}{2}(\epsilon - 1) - \frac{\kappa}{2}\beta\rho_i^2\right)\rho_i - \frac{2g^2}{9\Gamma}(\rho_{i+1}\cos(\theta_i - \theta_{i+1}) + \rho_{i-1}\cos(\theta_i - \theta_{i-1})), \quad (8.a)$$

and

$$\dot{\theta}_i = \omega_i + \frac{2g^2}{9\Gamma}\left(\frac{\rho_{i+1}}{\rho_i}\sin(\theta_i - \theta_{i+1}) + \frac{\rho_{i-1}}{\rho_i}\sin(\theta_i - \theta_{i-1})\right). \quad (8.b)$$

In the weak coupling limit, by increasing the coupling constant g to a critical value g_c^*, a phase lock exists between the lasers and the frequency synchronization occurs. The numerical investigations of equations (7 and 8) indicate that at the critical coupling g_c^*, each $\dot{\rho}_j = 0$, for $j = 1, 2, 3$, as well as the lasers' amplitudes become equal and time independent. Figure 3.a shows these previously noticed observations, where we plot the amplitudes and their time derivatives versus time at different values of g. Similarly, the numerical studies of $\dot{\theta}_j$ show that the time evolution of the lasers' phases at g_c^* demonstrating that all $\dot{\theta}_j = \omega_o$, for $j = 1, 2, 3$. According to plots (b – d) of figure (3), it noticed that there is an appeared synchronization at g_c, however the system is not stable at g_c. At g_c^*, all the three quantities $\dot{\theta}_j$ become time independent. Even if we start using equations (6 and 7) to perform the numerical examinations of the indirect coupled laser, we shall end up finding the same results when we employ relations of equations (8).

In the weak coupling regime, the detuning between the laser frequencies is small and the photon lifetime in the cold cavity is not larger than the laser photon lifetime. For large $\Gamma \gg 1$, the dominant terms on the r. h. s of any of the expressions (8.a) are the first terms. Henceforth, we safely set $\rho_j = \sqrt{(\epsilon - 1)/\beta}$. Consequently, the remaining dynamics of

the indirectly coupled lasers will be the phase dynamics and the time evolution of the phases are controlled by the phase differences quantities. Accordingly, equation (8.b) becomes

$$\dot{\theta}_{max} = \omega_{max} + \frac{2g^2}{9\Gamma}\left(\sin(\theta_{max} - \theta_m) + \sin(\theta_{max} - \theta_{min})\right),$$

$$\dot{\theta}_m = \omega_m + \frac{2g^2}{9\Gamma}\left(\sin(\theta_m - \theta_{max}) + \sin(\theta_m - \theta_{min})\right), \qquad (9)$$

$$\dot{\theta}_{min} = \omega_{min} + \frac{2g^2}{9\Gamma}\left(\sin(\theta_{min} - \theta_{max}) + \sin(\theta_{min} - \theta_m)\right),$$

which is the Kuramoto-like model [12, 13, 17, 18]. We can solve the Kuramoto-like model similar to the work in [17]. We find, for $\omega_{max} > \omega_o, \omega_m < \omega_o$ and $\omega_{min} < \omega_m$, that the phase difference at g_c^* is $\theta_m - \theta_{max} = -3\pi/2$. Thus, we find an analytic expression for g_c^* as

$$g_c^* = 3\sqrt{\frac{\Gamma}{2}\left((\omega_{max} - \omega_m) + \sqrt{2(\omega_{max} - \omega_o)(\omega_o - \omega_m)}\right)}. \qquad (10)$$

Use this above expression, we obtain analytic forms for the phase differences between each two lasers:

$$\theta_{max} - \theta_{min} = \sin^{-1}\left(\frac{(\omega_0 - \omega_m) - \sqrt{2}\sqrt{-((\omega_0 - \omega_{max})(\omega_0 - \omega_m))}}{(\omega_{max} - \omega_m) + \sqrt{2}\sqrt{-((\omega_0 - \omega_{max})(\omega_0 - \omega_m))}}\right), \qquad (11.a)$$

$$\theta_m - \theta_{min} = \sin^{-1}\left(\frac{(\omega_0 - \omega_{max}) - \sqrt{2}\sqrt{-((\omega_0 - \omega_{max})(\omega_0 - \omega_m))}}{(\omega_{max} - \omega_m) + \sqrt{2}\sqrt{-((\omega_0 - \omega_{max})(\omega_0 - \omega_m))}}\right). \qquad (11.b)$$

For the case of $\omega_{max} > \omega_0, \omega_m > \omega_0$ *and* $\omega_{min} < \omega_o$ we find the phase difference is $\theta_m - \theta_{min} = -3\pi/2$, and the critical coupling constant, g_c^*, takes the form:

$$g_c^* = 3\sqrt{\frac{\Gamma}{2}\left((\omega_m - \omega_{min}) + \sqrt{2(\omega_m - \omega_o)(\omega_o - \omega_{min})}\right)}. \qquad (12)$$

Therefore, the phase differences between each two lasers obey the following relations:

$$\theta_m - \theta_{max} = \sin^{-1}\left(\frac{(\omega_o - \omega_{min}) + \sqrt{2}\sqrt{-((\omega_m - \omega_o)(\omega_{min} - \omega_o))}}{(\omega_m - \omega_{min}) + \sqrt{2}\sqrt{-((\omega_m - \omega_o)(\omega_{min} - \omega_o))}}\right), \qquad (13.a)$$

$$\theta_{max} - \theta_{min} = \sin^{-1}\left(\frac{(\omega_m - \omega_o) - \sqrt{2}\sqrt{-((\omega_m - \omega_o)(\omega_{min} - \omega_o))}}{(\omega_m - \omega_{min}) + \sqrt{2}\sqrt{-((\omega_m - \omega_o)(\omega_{min} - \omega_o))}}\right). \qquad (13.b)$$

For a case when $\omega_m = \omega_o$, as shown in figure 3.d, the relations (10) and (12) give the value of the critical coupling g_c^*. In this case, the phase differences between each two lasers are given by the relations (11) and (13) and take the values: $\theta_{max} - \theta_m = \theta_m - \theta_{min} = 3\pi/2$, while $\theta_{max} - \theta_{min} = 3\pi$.

Conclusion:

In this work, we investigate systems of three lasers coupled to each other by two different connectivity methods. The direct coupling system exhibits a frequency

synchrony which spontaneously emerges when the coupling constant reaches a critical value. The direct coupling system reveals amplitudes and phases dependences. The indirect coupled case signifies a phase dependence only. The system in the second model is expressed by a Kuramoto-like model.

It is clear from the equation (3), the direct coupling system exhibits a frequency synchrony which spontaneously emerges when the coupling constant reaches a critical value according to amplitude and phase dependences. The unison behaviour appears upon repulsive interactions between lasers. This case is very interesting to be investigated in a more details. Although, the indirect coupling system appears a more complicated in comparison to the direct coupling case, we find a synchronous state at a critical coupling. Correspondingly, the system is described by a phase model only as given by equations (7 and 8). This description proves the fact that the system dynamics is explained in terms of the phases of each laser. We show how the system can be described by the Kuramoto-like model.

Systems (3) and (8) have Hamiltonian dynamics. It is possible to examine in more details the two systems of direct and indirect coupling starting from effective Hamiltonians [20 - 26]. These studies will illustrate quantitatively how the potential energy due to coupling leading to the dependence of the synchronization, in first model, on the amplitudes and phases. Also, we shall have more evidence, in correspondence to the second model, on how the synchrony appears only due to forces that come because of the additional potential energy due to coupling.

Declaration of Conflicting Interests

The author(s) declared no potential conflicts of interest concerning the research, authorship, and/or publication of this article.

References:

1. S. Strogatz, Nonlinear Dynamics and Chaos with Applications to Physics, Biology, Chemistry, and Engineering. 2nd Ed (CRC Press, New York, USA) (2018), https://doi.org/10.1201/9780429492563
2. S. Boccaletti, A. Pisarchik, C. Del Genio, A. Amann, Synchronization: From Coupled Systems to Complex Networks Cambridge: Cambridge University Press (2018), https://doi.org/10.1017/9781107297111
3. J. A. Acebrón, L. L. Bonilla, C. J. P. Ritort, R. Spigler, The Kuramoto Model: A Simple Paradigm for Synchronization Phenomena. Rev. Mod. Phys. 77 (2005)137, https://doi.org/10.1103/RevModPhys.77.137
4. T. A. Winfree, The geometry of biological time vol. 12. (Springer) 2001, https://doi.org/10.1007/978-1-4757-3484-3
5. T. P. Vinayak, P. B. Prosen, T. H. Seligman, Spectral analysis of finite-time correlation matrices near equilibrium phase transitions Euro. Phys. Lett. 108(2014) 20006, https://doi.org/10.1209/0295-5075/108/20006
6. H. Chang, Q. Chang, J. Xi, T. Hou, R. Su, P. Ma, J. Wu, C. Li, M. Jiang, Y. Ma, P. Zhou, First experimental demonstration of coherent beam combining of more than 100 beams, Photon. Res. 8(2020)1943-1948, https://doi.org/10.1364/PRJ.409788

7. D. Dudkowski, K. Czołczyński, T. Kapitaniak, Synchronization of two self-excited pendula: Influence of coupling structure's parameters, Mechanical Systems and Signal Processing 112 (2018)1-9, https://doi.org/10.1016/j.ymssp.2018.04.025

8. J. Fell and N. Axmacher, The role of phase synchronization in memory processes Nat. Rev. Neurosci. 12(2011)105, https://doi.org/10.1038/nrn2979

9. A. Motter, S. Myers, M. Anghel, T. Nishikawa, Spontaneous synchrony in power-grid networks. Nature Phys. 9(2013)191–197, https://doi.org/10.1038/nphys2535

10. M. B. Spencer, W. E. Lamb Jr, Theory of two coupled lasers, Phys. Rev. A. 5(1972) 893, https://doi.org/10.1103/PhysRevA.5.893

11. V. Pal, C. Tradonsky, C. Chriki, A. Friesem, N. Davidson, Observing Dissipative Topological Defects with Coupled Lasers, Phys. Rev. Lett. 119(2017)013902, https://doi.org/10.1103/PhysRevLett.119.013902

12. Y. Kuramoto, Chemical oscillations, waves, and turbulence (Berlin, Germany: Springer) (1984), https://doi.org/10.1007/978-3-642-69689-3

13. N. Takemura, K. Takata, M. Takiguchi, M. Notomi, Emulating the local Kuramoto model with an injection-locked photonic crystal laser array Sci. Rep.11(2021) 8587, https://doi.org/10.1038/s41598-021-86982-w

14. J. Ding, I. Belykh, A. Marandi, M. Miri, Dispersive versus Dissipative Coupling for Frequency Synchronization in Lasers, Phys. Rev. Applied 12(2019)054039, https://doi.org/ 10.1103/PhysRevApplied.12.054039

15. J. R. Tredicce, F. T. Arecchi, G. L. Lippi, G. P. Puccioni, Instabilities in lasers with an injected signal, JOSA B 2(1985)173, https://doi.org/10.1364/JOSAB.2.000173

16. P. R. Rice, H. J. Carmichael, Photon statistics of a cavity-QED laser: a comment on the laser-phase-transition analogy, Phys. Rev. A. 50(1994) 4318–4329, https://doi.org/10.1103/PhysRevA.50.4318

17. H. F. El-Nashar, Conditions and Linear Stability Analysis at The Transition to Synchronization of Three Coupled Phase Oscillators in A Ring, IJBC. 27(2017) 1750095(1-15), https://doi.org/10.1142/S021812741750095X

18. M. S. Mahmoud, H. F. El-Nashar, M. Medhat, Exact Solution of Four Coupled Nonidentical Kuramoto Oscillators at A Full Phase Locked State, IJBC. 33(2023)2350005, https://doi.org/10.1142/S0218127423500050

19. M. H. Latifpour, M. A. Miri, Mapping the XY Hamiltonian onto a network of coupled lasers, Phys. Rev. Res. 2(2020)043335, https://doi.org/10.1103/PhysRevResearch.2.043335

20. A. Politi, S. Yanchuk, G. Giacomelli, Nearly Hamiltonian dynamics of laser systems, Phys. Rev. Res 5(2023) 023059, https://doi.org/10.1103/PhysRevResearch.5.023059

21. G. Arwas, S. Gadasi, I. Gershenzon, A. Friesem, N. Davidson, O. Razet, Anyonic parity time symmetry in complex coupled lasers Sci. Adv .8(2022) eabm7454, https://doi.org/10.1126/sciadv.abm7454

22. I. E. Protsenko, A. V. Uskov, Oscillator Laser Model Ann. Phys. 535(2022) 2200298, https://doi.org/10.1002/andp.202200298

23. I. E. Protsenko, L. A. Lugiato, Laser generation with coloured input: I. Quantum Langevin equations for the laser. Quantum Semiclass. Opt. 8(1996) 1081, http://dx.doi.org/10.1088/1355-5111/8/5/012

24. D. Witthaut, S. Wimberger, R. Burioni, M. Timme, Classical synchronization indicates persistent entanglement in isolated quantum systems, Nat Commun 8(2017)14829, http://dx.doi.org/10.1038/s42005-024-01566-0

25. G. Chimczak, A. Kowalewska-Kudłaszyk, E. Lange, K. Bartkiewicz, J. Peřina Jr, The effect of thermal photons on exceptional points in coupled resonators, Sci Rep. 13(2023)5859, https://doi.org/10.1038/s41598-023-32864-2

26. I. Gonskov, S. Gräfe, Light–matter quantum dynamics of complex laser-driven systems, J. Chem. Phys. 154(2021)234106, https://doi.org/10.1063/5.0048930